CHEMISTRY
A EUROPEAN JOURNAL

DOI: 10.1002/chem.200600331

Continuous Symmetry Analysis of NMR Chemical Shielding Anisotropy

Avital Steinberg,[a, c] Miriam Karni,[b, c] and David Avnir*[a, c]

Abstract: Molecular symmetry is a key parameter which dictates the NMR chemical shielding anisotropy (CSA). Whereas correlations between specific geometrical features of molecules and the CSA are known, the quantitative correlation with symmetry—a global structural feature—has been unknown. Here we demonstrate a CSA/symmetry quantitative relation for the first time: We study how continuous deviation from exact symmetry around a nucleus affects its shielding. To achieve this we employed the continuous symmetry measures methodology, which allows one to quantify the degree of content of a given symmetry. The model case we use for this purpose is a population of distorted SiH_4 structures, for which we follow the ^{29}Si CSA as a function of the degree of tetrahedral symmetry and of square-planar symmetry. Quantitative correlations between the degree of these symmetries and the NMR shielding parameters emerge.

Keywords: chemical shifts · NMR spectroscopy · silicon · symmetry · tensors

Background

We study how continuous deviation from exact symmetry around a nucleus affects its nuclear magnetic resonance (NMR) chemical shielding anisotropy (CSA), a problem which is of relevance particularly to solid-state NMR studies.[1] Various relations between the components of the NMR shielding tensor have been shown to emerge from structural geometry considerations,[2] and these have been used to predict the CSA.[1] Yet an inherent problem has followed theoretical studies of NMR: While NMR theory is intimately linked to symmetry, the vast majority of molecules are not symmetric. A basic question then arises: How are characteristic NMR spectral parameters affected, when the molecule under study deviates from symmetry? In other words, when the molecule belongs to a certain point group, the relations between the shielding tensor components are known; but what happens to these relations when the molecule is distorted from this point group? And, how does a *gradual* symmetry distortion affect the gradual change in anisotropy? Consider for instance a tetracoordinated molecule, AB_4, once perfectly tetrahedral (T_d point group symmetry, Figure 1a), and then square-planar (D_{4h} symmetry, Figure 1b). The fact that these structures are of completely different symmetries is reflected in their shielding tensors: The tetrahedral structure can be placed in a frame of three geometrically equivalent axes and has therefore a perfectly isotropic shielding tensor and the CSA is zero. Of all possible conformations of an AB_4 molecule, the isotropic shielding is in fact the highest possible for the perfectly tetrahedral AB_4 molecule, since the symmetry around the central atom is the highest possible. On the other hand, the square-planar molecule can be placed in an axes frame so that two axes are equivalent and one is unique (Figure 1b). This molecule is geometrically anisotropic, since all of the B atoms

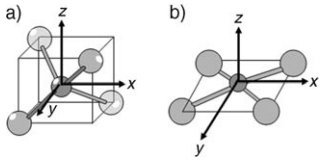

Figure 1. a) Perfect AB_4 tetrahedral molecule (T_d symmetry) is also perfectly isotropic and therefore perfectly shielded: x, y, and z directions are equivalent. b) Planar square AB_4 molecule (D_{4h} symmetry) is anisotropic: Its z direction (the "unique axis") is exposed, and the shielding is greatly reduced.

[a] A. Steinberg, Prof. D. Avnir
Institute of Chemistry, The Hebrew University of Jerusalem
Jerusalem 91904 (Israel)
Fax: (+972) 2-652-0099
E-mail: david@chem.ch.huji.ac.il

[b] Dr. M. Karni
Department of Chemistry
Technion—Israel Institute of Technology
Haifa 32000 (Israel)

[c] A. Steinberg, Dr. M. Karni, Prof. D. Avnir
The Lise Meitner Minerva Center for Computational Quantum Chemistry (at the Hebrew University and at the Technion)

are in the same plane and the z direction is exposed. Thus, for the D_{4h} molecule, anisotropy emerges. While the symmetry arguments for these two extreme cases is straightforward, there is a whole world of AB_4 molecules or molecular fragments, which are neither perfectly tetrahedral, nor perfectly planar square,[3,4] but have structures which are either of lower symmetry or even devoid of any symmetry altogether. In all of these structures—which are in fact, the vast majority of AB_4 species—the nucleus of A experiences, of course, some level of shielding anisotropy around it and yet under the current state of art of NMR studies, little, if at all, can be said about whatever relation there might exist between the reduced level of symmetry and the strength of the anisotropy. Consider a gradual distortion that a perfect tetrahedron undergoes until it becomes a square (Figure 2): When is it justified to stop considering the distorted tetrahedron as a T_d case for NMR purposes? After 5% distortion? After 0.5%? Or midway to the planar structure?

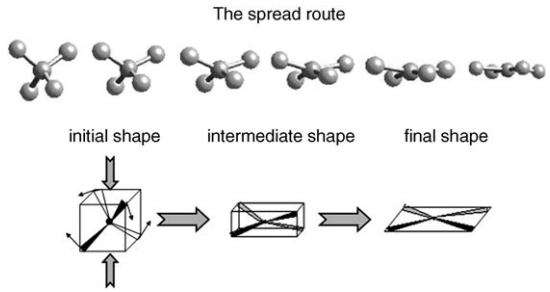

Figure 2. Top: Gradual transition of a tetrahedral molecule to a square-planar one. This is the "spread" distortion route that can be viewed (bottom) as the gradual compression of a cube in which the initial tetrahedron is captured.

It should be noted that changes in specific structural features such as bond lengths and angles have been correlated with NMR properties,[5–7] yet these do not solve the problem we pose, because the CSA is indeed affected by the symmetry around the relevant nucleus, namely by the whole array of all bond angles and bond lengths. Thus, a measurement tool for the degree of symmetry, a global parameter which encompasses all bonds and angles, is in need for CSA-symmetry correlations analysis. To address this question—as well as other many key symmetry-related issues in chemistry—we have advanced the notion of using a quantitative continuous scale for evaluating the degree of symmetry. The continuous symmetry measures (CSM) approach is briefly described in the next section, and indeed, as will be shown below, quantitative correlations between degree of symmetry and NMR shielding parameters emerge. We have used as a computational model the ^{29}Si NMR of distorted SiH_4 species (representing distortion during vibrational motions, due to adsorption or to other condensed-phase interactions, etc). While SiH_4 was selected as a convenient model for studying feasibility of the symmetry/NMR correlation analysis approach, we also had in mind to use it as a lead compound to more complex Si compounds studies in our research groups, and particularly to the solid state NMR of SiO_2 materials.[8]

Model and Computational Details

The continuous symmetry measure (CSM): The continuous symmetry measure of a structure is a (normalized root-mean-square) distance function from the closest structure which has the desired symmetry.[9–11] It is a special distance function which seeks the distance to a required symmetry, rather than to a preset reference structure (although on occasions the two coincide). Thus, it is a distance function to a structure that must be searched. Formally, given a (distorted) structure composed of N vertices (say, a central atom and the ligands attached to it), the coordinates of which are $\{A_k, k = 1, 2, \ldots, N\}$, one searches for the vertex coordinates of the nearest perfectly G-symmetric object, $\{\hat{A}_k, k = 1, 2, \ldots, N\}$. Once at hand, the symmetry measure is defined as:

$$S = \min \frac{\sum_{k=1}^{N} |A_k - \hat{A}_k|^2}{\sum_{k=1}^{N} |A_k - A_0|^2} \times 100 \quad (1)$$

where A_0 is the coordinates vector of the center of mass of the investigated structure

$$A_0 = \frac{1}{N} \sum_{k=1}^{N} A_k \quad (2)$$

The CSM defined in Equation (1) is independent of the position, orientation and size of the original structure. Equation (1) is general and allows one to evaluate the symmetry measure of *any* structure relative to *any* symmetry group G. To avoid size effects, the original structure is normalized to the r.m.s distance from the center of mass of the structure (placed at the origin) to all vertexes [the denominator in Eq. (1)]. The bounds are $100 \geq S \geq 0$, where $S(G) = 0$ means that the structure has the desired G symmetry. The symmetry measure increases as it departs from G symmetry and reaches a maximal value (not necessarily 100). All $S(G)$ values are on the same scale and are therefore comparable. The main practical problem is how to find the nearest structure that has the desired symmetry, namely $\{\hat{A}_k, k = 1, 2, \ldots, N\}$. Several algorithms have been developed in order to find the nearest symmetric object,[9–11] and we use here the algorithms described in ref. [11].

The CSM methodology has been applied successfully to many symmetry related problems in physics, chemistry, biochemistry and spectroscopy, and some examples are collected in references [4,12–17]. Of relevance to this report are the relationships between octahedricity or trigonal prismacity, and the magnetic moment within a family of related spin crossover complexes, which were found by Alvarez to be in-

dependent of the nature of the external perturbations applied;[12] the correlations between the CSM and electron spin resonance;[17] and between the degree of symmetry and electronic spectral transition energies and probabilities.[17]

The symmetry-distorted molecules

The randomly distorted structures: In order to determine possible correlations with symmetry—not with specific geometrical features—it was necessary to create a population in which the symmetry around the nucleus is random. Thus, a population of 200 randomly distorted SiH_4 structures was created for which the tetrahedral angles were selected randomly but kept between 90–180°, representing the actual range of A-Si-A angles found in various Si compounds.[18] Since the experimental variability in Si–H bond lengths is small, these where kept constant (1.48 Å;[19] the $S(G)$ values change only very little if some randomness is allowed here as well).

The "spread route" structures: Complementary to the randomly distorted population would be a series of homologous structures the distortion of which changes gradually and in a predetermined way. For this purpose the gradual transition from a perfect tetrahedron (T_d) to a planar square (D_{4h})—the highest possible symmetry point groups for AB_4 structures—along a common distortion route known as the "spread route" (Figure 2), was selected.[17,20,21] Note that a characteristic of the spread route is that it maintains a D_2 axial symmetry throughout. 23 equally-spaced structures along that route were taken.[22] An important observation has been that the spread planarization path[17,21] relates maximal symmetry (see below) with minimal energy.[4]

NMR computations: As for computation of the CSA, we recall that its orientational dependence is expressed by a 3-by-3 chemical shielding tensor, the diagonalization of which provides the three principle components of the shielding tensor—σ_{11}, σ_{22}, σ_{33}, defined as the largest, the medium and the smallest components, respectively. For most molecules, the three components are not equal, and the chemical shielding becomes anisotropic. This anisotropy is traditionally expressed through the CSA:

$$\mathrm{CSA} = \sigma_{11} - \tfrac{1}{2}(\sigma_{22} + \sigma_{33}) \qquad (3)$$

It can be seen that for a perfect tetrahedron (Figure 1a), CSA = 0. For a square-planar molecule (Figure 1b) the shielding tensor is axially symmetric, namely σ_{11} is unique and the two others are equal. The NMR parameters of the ^{29}Si nucleus were calculated using Gaussian 98[23,24] at the B3LYP/6-31G* level.[25a] (Since the shielding tensor should not depend on an arbitrarily chosen origin, a gauge independent method (the gauge invariant atomic orbital (GIAO) method) was used,[25b] in which the explicit field-dependence is built into the atom-centered basis functions.) It should be noted that despite being a small basis set (identification of trends were more important to us than "true" values at this stage), its selection gave very satisfactory results: The experimental value of ^{29}Si in SiH_4 for σ_{iso} is 475.3 ± 10 ppm,[26] whereas the B3LYP/6-31G* calculation gave $\sigma_{iso} = 484.24$ ppm, which is within the error range of the experimental result.[27]

Results and Interpretations

The analyzed structures: Before entering the symmetry/CSA relations, it is in order to comment on the random population of the distorted SiH_4 structures formed as described above. Given a random arrangement of four B ligands around a central A atom, one can ask "what is the tetrahedricity content, $S(T_d)$, of AB_4?". However, since many differently distorted structures can have the same $S(T_d)$ values (recall that the symmetry measure is a thermodynamic-like global characterization parameter), it was found very useful to characterize the symmetry content more uniquely by analyzing the distance of AB_4 from the *two* highest possible symmetry point groups, which are not sub-groups of each other. For an AB_4 structure these symmetries are, as mentioned above, T_d and the planar D_{4h}. Having the two parameters $S(D_{4h})$ and $S(T_d)$ at hand, one can then draw a "symmetry map", namely a plot of $S(D_{4h})$ versus $S(T_d)$ for the various AB_4 structures under study. Symmetry maps proved to be quite powerful in analyzing various symmetry deviations of various families of molecules.[28] Let us then observe

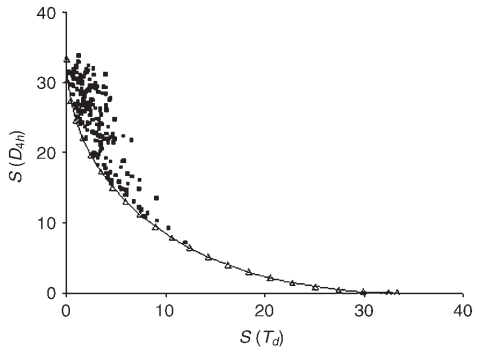

Figure 3. "Symmetry map" of the studied structures. Plotted is the degree of square-planarity versus the degree of tetrahedricity for each structure. Squares: The random population; triangles connected by line: Spread structures.

the symmetry map of the structures we analyze (Figure 3): First, it is seen that the Spread structures span from perfect tetrahedricity, namely $S(T_d) = 0$ (and there is still some degree of planarity in it, which is $S(D_{4h}) = 33.33$) to perfect planarity ($S(D_{4h}) = 0$; $S(T_d) = 33.33$). The full route from tetrahedricity to planarity exists here, simply because each structure was built by choice. On the other hand, the collection of 200 structures was imposed by the random selection rules, and it is clearly seen that the majority of structures

are nearer to tetrahedral than to planar. This is not surprising—the chance of hitting a 2D-planar or nearly planar structure are very low (only in symmetry maps which contain thousands of random structures are they obtained,[28] and the chances of spreading the H atoms around the Si in a 3D fashion are much higher. (In fact, note that the chance of hitting an exact tetrahedral structure is likewise very low—indeed, there is none in Figure 3.)

Next note that the spread structures form the lower bound of the random population. That lowest bound means that upon conversion of a tetrahedron to a planar species, that route is the most symmetric one from the point of view that each of the points on it is characterized by the lowest possible pair of $S(T_d)/S(D_{4h})$ values.[17,21] Indeed, we shall see this extreme behavior also in the CSA analysis of this group of structures.

The CSA-symmetry correlations: Intuitively one expects to find that with increase of deviation from tetrahedral symmetry, the CSA will increase (keeping in mind that the minimal anisotropy is that for the perfect tetrahedron). Figure 4 successfully translates this qualitative intuition into a quantitative relation and shows how the CSA of ^{29}Si increases with $S(T_d)$. This observation is non-trivial for the following reason: Recall that the symmetry measure is a global, overall shape parameter and not a specific structural one, and so what one sees in Figure 4 is a true response to symmetry changes and not to a specific geometric feature. To the best of our knowledge this type of correlation has not been identified so far in the NMR literature. If the trend in Figure 4 is authentic, then a plot of the CSA as a function of planarity should produce an opposite trend, because the highest anisotropy, as explained above, is for the perfect planar square; Figure 5 shows that this is indeed the case.

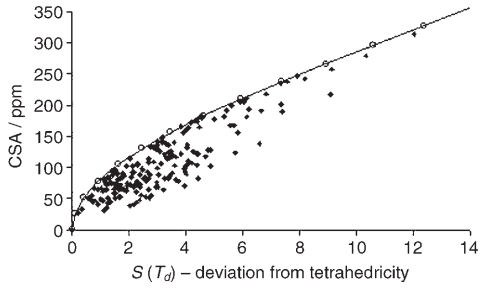

Figure 4. Chemical shielding anisotropy of ^{29}Si is plotted against the degree of tetrahedral symmetry of the random SiH_4 structures (deviation from tetrahedricity increases from left to right); shown also are the spread structures (top line).

Interestingly, as seen in Figures 4 and 5 the spread structures appear at the extrema of the random populations analyses: At the maximum of the $S(T_d)$ analysis (Figure 4), but at the minimum of the correlation with $S(D_{4h})$ (Figure 5); that is, the spread structures define the limits of the correlation between the CSA and the high symmetries. To understand these observations we recall that the spread structures—as explained above—are minimally distorted from both tetrahedricity and planarity, that is, they have a minimal pair of $S(T_d)/S(D_{4h})$ values.[17,21] Consider, for instance all molecules bearing the same $S(D_{4h})$ value (a vertical cross-section in Figure 5). A structure which belongs to the spread family and which resides on that cross section will have the minimal possible $S(T_d)$ value for that selected $S(D_{4h})$ value, and therefore *also* the minimal anisotropy; hence the existence of the spread line at the minimum of Figure 5. A similar argument explains why that line is at the maximum of Figure 4: Any structure on that line has the maximal possible degree of planarity, and hence also the maximal anisotropy.

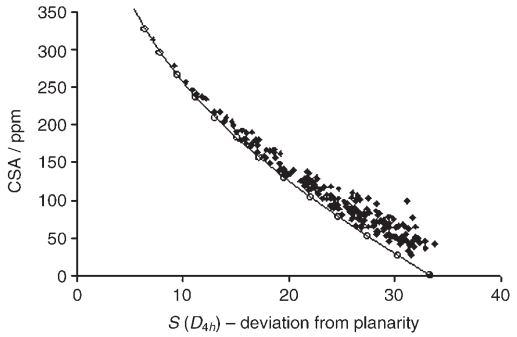

Figure 5. CSA versus degree of square-planarity. The trend here is reversed compared with that of the previous figure, and the spread structures appear as the lower bound.

Next, it is also interesting to analyze the symmetry sensitivity of the three shielding tensors components, from which the CSA is composed, and we take the $S(T_d)$ for this analysis. The governing effect of the σ_{11} component is clearly evident in Figure 6.[29] Note that all components start at the same point, since for a perfect tetrahedron, $\sigma_{11}=\sigma_{22}=\sigma_{33}$, and, as the tetrahedron is distorted, the shielding along the different axes is no longer uniform, and the behavior of the tensors splits; the maximal shielding component σ_{11} rises, σ_{33}

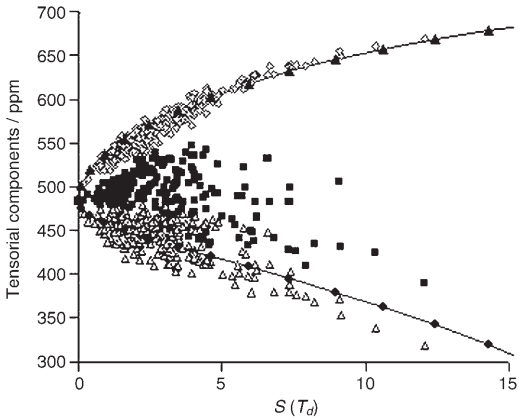

Figure 6. Three tensor components versus $S(T_d)$. For the perfect tetrahedron, all three components are equal; as the tetrahedron is distorted, the components gradually separate. Random population: σ_{11} (◇), σ_{22} (■), σ_{33} (△); spread population: σ_{11} (▲), σ_{22} (◆).

decreases, while σ_{22} is scattered in between. As we have seen in Figure 4, the CSA increases as the tetrahedron is distorted. Since the CSA is the difference between the largest component and the average of the other two, one would indeed expect to see the CSA dictated by σ_{11}. Notice also that unlike the CSA behavior, the lines of the spread tensor components for σ_{11} and σ_{22} $(=\sigma_{33})$[30] are not at the edges of the random structures domains. To understand the difference between the CSA and the tensors behavior from that point of view, we recall that the symmetry analysis is global, that is, it treats the molecule as a whole as is the case for the CSA, and therefore, an extremum in one is also an extremum in the other; tensorial analysis, on the other hand, splits this globality into components, and therefore this joint-extrema argument does not hold in this case.

Conclusion

A quantitative correlation between symmetry as a global structural feature and NMR anisotropic shielding parameters was shown for the first time. Since the symmetry distortions were random, the correlations found indeed do not represent specific geometry changes, but symmetry per se. A group of structures which belong to the common Spread distortion mode, exhibits extreme behavior with regards to its NMR parameters.

Programs Availability

CSM programs, as well as chirality measurement programs, are free for use by writing to the authors.

[1] E. Klaus, A. Sebald, *Magn. Reson. Chem.* **1994**, *32*, 679–690; W. A. Dollase, M. Feike, H. Forster, T. Schaller, I. Schnell, A. Sebald, S. Steuernagel, *J. Am. Chem. Soc.* **1997**, *119*, 3807–3810.
[2] A. D. Buckingham, S. M. Malm, *Mol. Phys.* **1971**, *22*, 1127–1130.
[3] J. Cirera, P. Alemany, S. Alvarez, *Chem. Eur. J.* **2004**, *10*, 190–207.
[4] S. Keinan, D. Avnir, *Inorg. Chem.* **2001**, *40*, 318–323.
[5] A. R. Grimmer, R. Peter, E. Fechner, G. Molgedey, *Chem. Phys. Lett.* **1981**, *77*, 331–335.
[6] A. R. Grimmer, R. Radeglia, *Chem. Phys. Lett.* **1984**, *106*, 262–265.
[7] A. R. Grimmer, *Chem. Phys. Lett.* **1985**, *119*, 416–420.
[8] D. Yogev-Einot, D. Avnir, *Chem. Mater.* **2003**, *15*, 464–472.
[9] H. Zabrodsky, S. Peleg, D. Avnir, *J. Am. Chem. Soc.* **1992**, *114*, 7843–7851.
[10] H. Zabrodsky, S. Peleg, D. Avnir, *J. Am. Chem. Soc.* **1993**, *115*, 8278–8289.
[11] M. Pinsky, D. Avnir, *Inorg. Chem.* **1998**, *37*, 5575–5582.
[12] S. Alvarez, *J. Am. Chem. Soc.* **2003**, *125*, 6795–6802.
[13] P. L. Alonso, J. Fornies, M. A. Garcia-Monforte, A. Martin, B. Menjon, *Chem. Eur. J.* **2005**, *11*, 4713–4724.
[14] D. M. Jenkins, J. C. Peters, *J. Am. Chem. Soc.* **2005**, *127*, 7148–7165.
[15] K. D. Kanis, J. C. Wong, T. S. Mark, M. A. Ratner, H. Zabrodsky, S. Keinan, D. Avnir, *J. Phys. Chem.* **1995**, *99*, 11061–11066.
[16] S. Keinan, D. Avnir, *J. Am. Chem. Soc.* **2000**, *122*, 4378–4384.
[17] S. Keinan, D. Avnir, *J. Chem. Soc. Dalton Trans.* **2001**, 941–947.
[18] V. Moravetski, J. Hill, U. Eichler, A. K. Cheetham, S. J. Joachim, *J. Am. Chem. Soc.* **1996**, *118*, 13015–13020.
[19] J. E. Huheey, *Inorganic Chemistry: Principles of Structure and Reactivity*, 3rd ed., Harper and Row, **1983**.
[20] W. Luef, R. Keese, *J. Mol. Struct.* **1992**, 353–368.
[21] D. Casanova, J. Cirera, M. Llunell, P. Alemany, D. Avnir, S. Alvarez, *J. Am. Chem. Soc.* **2004**, *126*, 1755–1763.
[22] With constant bond lengths of 1.48 Å.
[23] W. Koch, A. Holthausen, *A Chemist's Guide to Density Functional Theory*, 2nd ed., Wiley VCH, **2002**.
[24] Gaussian 98, Revision A.11.3, M. J. Frisch, G. W. Trucks, H. B, Schlegel, G. E. Scuseria, M. A. Robb, J. R. Cheeseman, V. G. Zakrzewski, J. A. Montgomery, R. E. Stratmann, J. C. Burant, S. Dapprich, J. M. Millam, A. D. Daniels, K. N. Kudin, M. C. Strain, O. Farkas, J. Tomasi, V. Barone, M. Cossi, R. Cammi, B. Mennucci, C. Pomelli, C. Adamo, S. Clifford, J. Ochterski, G. A. Petersson, P. Y. Ayala, Q. Cui, K. Morokuma, N. Rega, P. Salvador, J. J. Dannenberg, D. K. Malick, A. D. Rabuck, K. Raghavachari, J. B. Foresman, J. Cioslowski, J. V. Ortiz, A. G. Baboul, B. B. Stefanov, G. Liu, A. Liashenko, P. Piskorz, I. Komaromi, R. Gomperts, R. L. Martin, D. J. Fox, T. Keith, M. A. Al Laham, C. Y. Peng, A. Nanayakkara, M. Challacombe, P. M. Gill, B. Johnson, W. Chen, M. W. Wong, J. L. Andres, C. Gonzalez, M. Head Gordon, E. S. Replogle, J. A. Pople, Gaussian Inc., Pittsburgh, **2002**.
[25] a) A. D. Becke, *J. Chem. Phys.* **1993**, *98*, 5648–5652; b) K. Wolinski, J. F. Hinton, P. Pulay, *J. Am. Chem. Soc.*, **1990**, *112*, 8251–8260.
[26] C. J. Jameson, *Chem. Phys. Lett.* **1988**, *149*, 300–305.
[27] The HF/6-31G* calculation gave a σ_{so} of 519 ppm, which is quite far from the experimental result. The MP2/6-31G* gave an even worse result: $\sigma_{iso}=524$ ppm.
[28] S. Alvarez, P. Alemany, D. Casanova, J. Cirera, M. Llunell, D. Avnir, *Coord. Chem. Rev.* **2005**, *249*, 1693–1708.
[29] σ_{11}, the unique tensor is the largest by definition, and is aligned along the z axis for the spread population. σ_{22} and σ_{33} are perpendicular to it.
[30] Due to the D_2 symmetry of the spread structures, $\sigma_{22}=\sigma_{33}$, coinciding with the x,y axes. σ_{11}, the unique tensor, coincides with the z axis.

Received: March 9, 2006
Published online: September 1, 2006

